Introduction

Hepatitis C virus (HCV) infection is one of the major causes of chronic hepatitis, which progresses to hepatocellular carcinoma (HCC) in many patients [1]. In the last two decades, interferon (IFN) therapy has been used to treat chronic hepatitis C (CH-C) with the goal of altering its natural progression. Although HCV eradication with IFN therapy in CH-C patients reportedly prevents HCC development [2–4], factors responsible for HCC development in IFN-treated patients are difficult to determine because of the prolonged clinical course of CH-C.

Recent studies demonstrated that single nucleotide polymorphisms (SNPs) near *interleukin (IL) 28B* were strongly associated with the virological response to pegylated IFNα (PEG-IFNα) and ribavirin (RBV) combination therapy [5–7]. However, it remains unclear if the SNPs near *IL28B* are associated with further consequences of CH-C, such as HCC and liver fibrosis, in IFN-treated patients because of the paucity of adequate cohort studies. To address the important question of whether SNPs near *IL28B* are associated with the development of HCC, we analyzed the influence of this polymorphism on HCC risk in a large-scale, long-term cohort of IFN-treated patients.

Methods

Patients

Patients chronically infected with HCV who had histologically proven chronic hepatitis or cirrhosis and had undergone IFN treatment between 1992 and 2010 were enrolled in the original cohort [8]. In this cohort comprising 1,818 patients, a subgroup of 792 patients who were available for genotyping of the SNPs near *IL28B* (rs8099917 and rs12979860) was assessed in the present study. Patients were excluded from the original cohort if they had a history of HCC at the time of liver biopsy, autoimmune hepatitis, primary biliary cirrhosis, excessive alcohol consumption (≥50 g/day), hepatitis B surface antigen, or anti-human immunodeficiency virus antibody. HCC was definitively ruled out by ultrasonography, dynamic computed tomography (CT), and/or magnetic resonance imaging (MRI) on enrollment. Written informed consent was obtained from all patients, and the Ethical Committee of Musashino Red Cross Hospital approved this study, which was conducted in accordance with the Declaration of Helsinki.

Genotyping for SNPs near *IL28B* (rs8099917 and rs12979860)

Genetic polymorphisms in tagged SNPs located near *IL28B* (rs8099917 and rs12979860) were determined by direct sequencing of PCR-amplified DNA, as reported previously [9].

Histological evaluation

Laparoscopic or ultrasound-guided liver biopsy was undertaken using 13-gauge or 15-gauge needles, respectively. The median length of specimens was 18 mm (range 11–40 mm), and the median number of portal tracts was 18 (range 9–34). Fibrosis stage and grade of inflammatory activity were scored by two pathologists according to Desmet et al.'s classification [10]. In case of interobserver disagreement in histological staging or grading, the diagnosis was confirmed by consensus.

IFN therapy and definitions of response to IFN therapy

All patients had chronic HCV infection at liver biopsy, which was confirmed by the presence of HCV-RNA in serum. All IFN therapies were initiated within 48 weeks after liver biopsy. Of 792 patients, 71 patients received IFNα or IFNβ monotherapy for 24 weeks, 54 received IFNα/RBV combination therapy for 24 weeks, 118 received PEG-IFNα monotherapy for 48 weeks, and 549 received PEG-IFNα/RBV combination therapy for 48–72 weeks.

Patients negative for serum HCV-RNA 24 weeks after IFN therapy completion were defined as sustained virological responders (SVRs). Patients who remained positive for HCV-RNA 24 weeks after therapy completion were defined as nonSVRs. HCV-RNA was determined by the qualitative Amplicor or TaqMan HCV assay (Roche Molecular Diagnostics, Tokyo, Japan).

Data collection and patient follow up

At primary liver biopsy, patient characteristics and biochemical, hematological, virological, and histological data were evaluated. Age at primary liver biopsy was determined. Patients were examined for HCC by abdominal ultrasonography, dynamic computed tomography, and/or magnetic resonance imaging every 3–6 months. Serum alanine aminotransferase (ALT) and α-fetoprotein (AFP) levels were measured every 1–6 months. Surveillance protocols were in accordance with the standard of care in Japan. If HCC was suspected on the basis of the screening examination, additional procedures (e.g., dynamic CT, dynamic MRI, CT during hepatic arteriography, CT during arterial portography, contrast-enhanced ultrasonography, and tumor biopsy) were used to confirm the diagnosis. HCC diagnosis was confirmed by needle biopsy, histology of surgically resected specimens, or characteristic radiological findings. To evaluate the effect of changes in serum ALT and AFP levels during IFN therapy on

hepatocarcinogenesis, mean integration values of ALT and AFP in each patient were calculated before and after IFN therapy. In patients who developed HCC, data obtained more than 1 year prior to HCC development were used to exclude AFP elevation caused by HCC itself.

Follow-up was between the date of primary liver biopsy and HCC development or the last medical attendance until June 2011. The mean follow-up period was 4.9 years (range 1.0–18.6 years).

Determination of changes in fibrosis stage over time

Changes in fibrosis stage over time were determined in patients who showed evidence of a single blood transfusion as a known time of HCV infection. Two hundred ninety-four patients had a single blood transfusion before 1992, indicating the known time of HCV infection (rs8099917 TT, $n = 217$; rs8099917 nonTT, $n = 77$). In this subgroup, 221 (75.2 %) patients were infected with HCV genotype 1. Annual fibrosis progression rate (FPR) was calculated as the fibrosis stage at liver biopsy divided by HCV infection duration, which was determined by the period between blood transfusion and liver biopsy (mean duration, 35.1 years; range 12.0–60.0 years).

Statistical analyses

Categorical data were compared by Chi-square or Fisher's exact tests. Continuous variable distributions were analyzed with Student's *t*- or Mann–Whitney *U* test. All tests of significance were two-tailed. $p < 0.05$ was considered significant. The cumulative incidence curve was determined by the Kaplan–Meier method, and differences between groups were assessed using the logrank test. Factors associated with HCC risk were determined by the Cox proportional hazard model. As covariates in the multivariate stepwise Cox model, age, sex, stage of liver fibrosis, pre- and post-IFN treatment ALT and AFP levels, virological response, and *IL28B* genotype were included. HCC development was the dependent variable. Time zero was defined as the time of primary liver biopsy. The proportional assumption was supported by log[−log(survival)] vs. log(time) plots, which showed parallel lines. Statistical analyses were performed using the Statistical Package for the Social Sciences software (version 18.0) (SPSS Inc., Chicago, IL, USA).

Results

Patient characteristics and the SNPs near *IL28B*

Patient characteristics are demonstrated in Table 1. Frequency of the rs8099917 genotype was as follows: major homozygote (TT), 74.2 % (588/792); heterozygote (TG), 24.2 % (192/792); and minor homozygote (GG), 1.5 % (12/792). Genotypic distribution of this SNP was consistent with that in a recent report on Japanese patients [5]. The frequency of the rs12979860 genotype was as follows: major homozygote (TT), 73.4 % (581/792); heterozygote (TG), 25.1 % (199/792); and minor homozygote (GG), 1.5 % (12/792). The genotypic discrepancy between rs8099917 and rs12979860 was found only in seven patients. Therefore, the genotypes of the two SNPs (rs8099917 and rs12979860) were 99.1 % identical. All seven patients had a major homozygote (TT) in rs8099917 but a heterozygote (CT) in rs12979860, and HCC developed in one of seven patients at 2.2 years after initiation of the follow-up.

Response to IFN therapy

The final responses to IFN therapy (SVR or nonSVR) were determined in all patients. SVR rate was significantly higher in TT patients than in nonTT patients (58.3 vs. 27.9 %, $p < 0.001$) (Table 1). SVR rates for each therapeutic regimen in TT and nonTT patients, respectively, were as follows: IFN monotherapy, 35.7 % (20/56) vs. 26.7 % (4/15), $p = 0.759$; IFNα/RBV combination therapy, 46.3 % (19/41) vs. 15.4 % (2/13), $p = 0.057$; PEG-IFNα monotherapy, 63.2 % (55/87) vs. 35.5 % (11/31), $p = 0.008$; PEG-IFNα/RBV combination therapy, 61.6 % (249/404) vs. 27.6 % (40/145), $p < 0.001$.

Factors associated with the SNPs near *IL28B*

NonTT patients were significantly associated with higher γ-glutamyl transpeptidase levels, lower low-density lipoprotein cholesterol levels, higher hepatic steatosis frequency, glutamine or histidine mutations at amino acid position 70 (70QH) in the HCV core region, and one or no mutation in the IFN sensitivity-determining region in the HCV nonstructural 5A gene (Table 1).

Cumulative incidence of HCC according to the SNPs near *IL28B*

During follow-up, 53 patients developed HCC (Table 1). At 3, 5, and 10 years, the overall cumulative incidence of HCC was 3.4, 7.4, and 13.1 %, respectively. The cumulative incidence of HCC at 5 and 10 years was significantly higher in nonTT patients than in TT patients (13.0 and 20.8 % vs. 5.4 and 10.5 %, respectively; logrank test, $p = 0.002$) (Fig. 1a). Among SVRs, no significant difference was found in the cumulative HCC incidence between TT and nonTT patients (Fig. 1b). However, the cumulative incidence of HCC among nonSVRs was significantly

Table 1 Characteristics of patients and comparison between the SNPs near *IL28B*

Characteristics	Total	rs8099917 TT	rs8099917 nonTT	*p* value*
Patients, *n*	792	588	204	
Sex, *n* (%)				0.329†
Male	310 (39.1)	236 (40.1)	74 (36.3)	
Female	482 (60.9)	352 (59.9)	130 (63.7)	
Age (SD), year	58.6 (10.7)	58.5 (10.6)	58.8 (11.0)	0.684‡
BMI (SD), kg/m^2	22.8 (3.2)	22.9 (3.2)	22.7 (3.3)	0.382‡
Fibrosis stage, *n* (%)				0.751†
F1/2	612 (77.3)	456 (77.6)	156 (76.5)	
F3/4	180 (22.7)	132 (22.4)	48 (23.5)	
%Severe steatosis (≥10%)	25.3	21.4	35.4	<0.001†
ALT level (SD), IU/L	63.4 (52.5)	64.9 (50.1)	59.0 (42.9)	0.170‡
γ-GTP level (SD), IU/L	45.9 (45.3)	41.5 (43.5)	58.3 (47.9)	<0.001‡
LDL-C level (SD), mg/dL	99.8 (26.8)	102.0 (26.6)	93.6 (26.8)	0.034‡
AFP level (SD), ng/mL	10.3 (26.7)	8.24 (12.2)	16.4 (47.9)	<0.001‡
Platelet counts (SD), $\times 10^3/\mu L$	164 (52)	163 (51)	167 (56)	0.422‡
HCV load (SD), KIU/mL	1550 (1465)	1612 (1465)	1392 (1457)	0.107‡
HCV genotype, *n* (%)[a]				0.065†
1a	8 (1.0)	5 (0.9)	3 (1.5)	
1b	588 (74.8)	422 (72.4)	166 (81.7)	
2a	118 (15.0)	96 (16.5)	22 (10.8)	
2b	63 (8.0)	52 (8.9)	11 (5.4)	
Others	9 (1.1)	8 (1.4)	1 (0.5)	
%Core 70 a.a. mutation[b]	34.5	26.2	57.1	<0.001†
%ISDR wild or 1 mutation[c]	67.4	64.0	76.1	0.005†
Duration (SD), year	4.9 (3.0)	5.0 (3.1)	4.8 (2.8)	0.480‡
IFN regimen, *n* (%)				0.798†
IFN mono	71 (9.0)	56 (9.5)	15 (7.4)	
IFN + RBV	54 (6.8)	41 (7.0)	13 (6.4)	
PEG-IFN mono	118 (14.9)	87 (14.8)	31 (15.2)	
PEG-IFN + RBV	549 (69.3)	404 (68.7)	145 (71.1)	
SVR, *n* (%)	400 (50.5)	343 (58.3)	57 (27.9)	<0.001†
HCC, *n* (%)	53 (6.7)	30 (5.1)	23 (11.3)	0.002†

* Comparison between *IL28B* major and minor genotypes

† Chi-square test

‡ Student's *t*-test

[a] HCV genotype was determined in 786 patients (*n*: *IL28B* major = 583, minor = 203)

[b] HCV core mutation was determined in 313 patients with genotype 1b

[c] ISDR was determined in 585 patients with genotype 1b

higher in nonTT patients than in TT patients (15.5, and 24.8 vs. 7.2 %, and 15.4 % at 5, and 10 years, respectively; logrank test, $p = 0.016$) (Fig. 1c). Similar results were obtained when the rs12979860 genotype was used as a reference. That is, the cumulative incidences of HCC at 5 and 10 years in overall patients were 13.1 and 20.5 % in nonCC patients and 5.2 and 10.4 % in CC patients (logrank test, $p = 0.001$); those in SVRs were 3.8 and 4.9 % in CC patients and 4.9 and 4.9 % in nonCC patients; and those in nonSVRs were 15.9 and 25.1 % in nonCC patients and 6.8 and 15.0 % in CC patients (logrank test, $p = 0.008$).

Ten subjects [rs8099917 TT, $n = 9$; nonTT, $n = 1$: SVR, $n = 8$; nonSVR, $n = 2$: mean follow-up period = 4.3 years (range 1.1–8.3 years)] were lost to follow-up during the last 2 years. These patients were censored from the cumulative incidence analyses at the time of the last visit.

In this study cohort, only three (one TT, $n = 1$; nonTT, $n = 2$) patients died during follow-up, and no patient underwent liver transplantation. These deaths were HCC-related. Therefore, it is unlikely that competing risks would have affected our results regarding differences in HCC incidence between TT and nonTT patients.

Because the SNPs near *IL28B* affects treatment responses particularly in patients infected with HCV genotype 1 and/or those treated with PEG-IFNα/RBV combination therapy, the cumulative incidences of HCC were analyzed in a subgroup of the patients. In patients infected with HCV genotype 1 ($n = 596$), the cumulative incidence of HCC was significantly higher in nonTT patients than in TT patients (15.2 and 24.9 % vs. 6.4 and 10.5 % at 5, and 10 years, respectively; logrank test, $p = 0.001$) (Fig. 1d). In patients treated with PEG-IFNα/RBV combination therapy ($n = 549$), the cumulative incidence of HCC was also

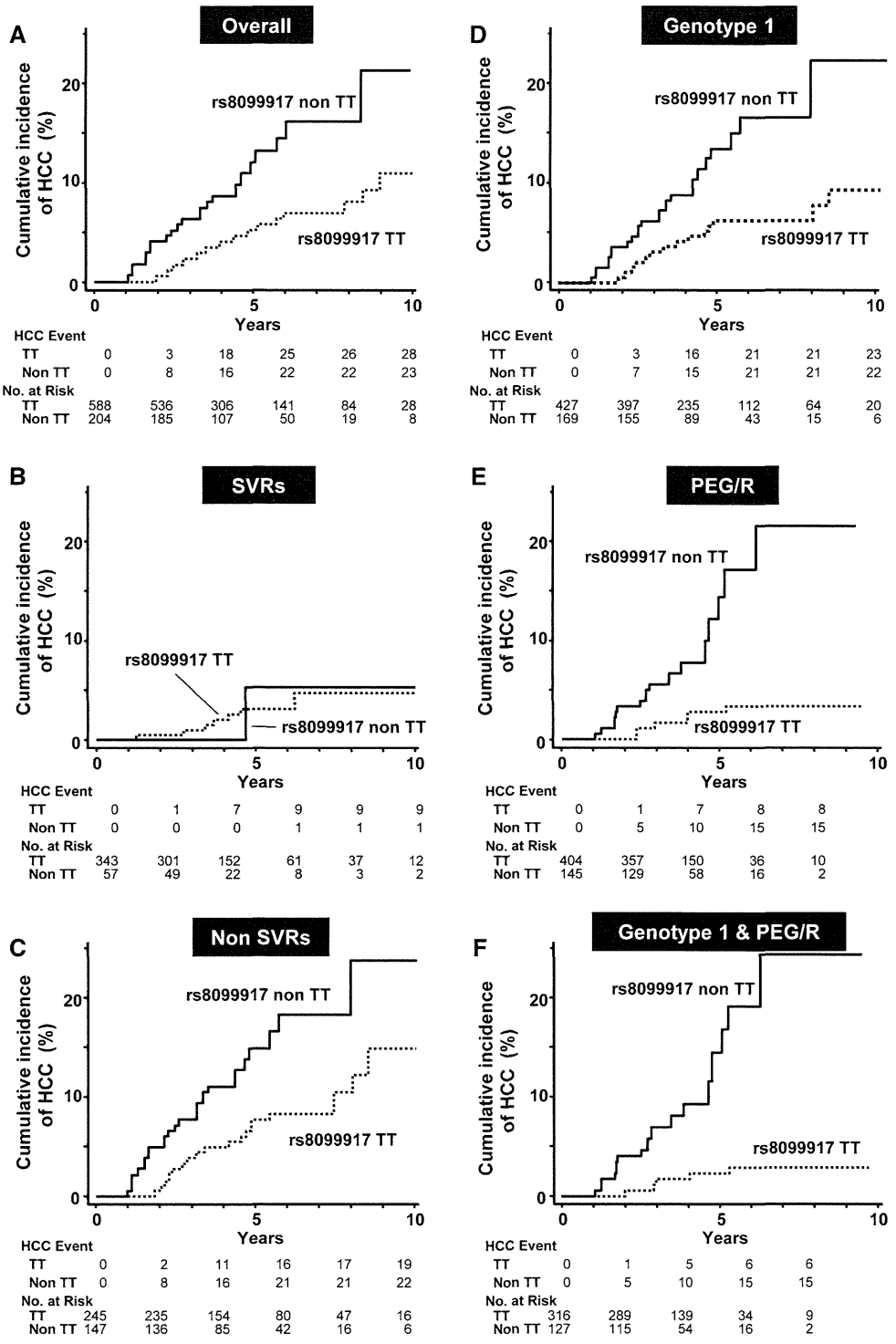

Fig. 1 Cumulative incidence of HCC according to genetic variation near *IL28B*. **a** Data for the entire patient group. Logrank test: $p = 0.002$. **b** Data for SVRs. Logrank test: $p = 0.775$. **c** Data for nonSVRs. Logrank test: $p = 0.016$. **d** Data for patients with HCV genotype 1. Logrank test: $p = 0.001$. **e** Data for patients who were treated with PEG-IFNα/RBV combination therapy. Logrank test: $p < 0.001$. **f** Data for patients with HCV genotype 1 who were treated with PEG-IFNα/RBV combination therapy. Logrank test: $p < 0.001$

significantly higher in nonTT patients than in TT patients (17.9, and 22.7 vs. 2.6, and 3.6 % at 5, and 9 years, respectively; logrank test, $p < 0.001$) (Fig. 1e). Particularly, in patients infected with HCV genotype 1 who were treated with PEG-IFNα/RBV ($n = 443$), the cumulative incidence of HCC was significantly higher in nonTT patients than in TT patients (19.5, and 24.5 vs. 2.2, and 3.2 % at 5, and 9 years, respectively; logrank test, $p < 0.001$) (Fig. 1f). Among patients infected with HCV genotype non-1 or those treated with other than PEG-IFNα/RBV therapy, no significant difference was found in the cumulative HCC incidence between TT and nonTT patients.

Influence of the SNPs near *IL28B* on progression of fibrosis over time

Among the 294 patients with evidence of a single blood transfusion, the annual FPR was similar between TT and nonTT patients ($p = 0.758$, Fig. 2). No difference was found in age at blood transfusion (26.0 [SD, 9.7] years old vs. 26.5 [SD, 9.6] years old, $p = 0.658$) and duration of HCV infection (34.7 [10.0] years vs. 36.1 [9.9] years, $p = 0.291$) between TT and nonTT patients.

Mean ALT and AFP levels after IFN therapy according to the SNPs near *IL28B*

Because we recently reported that post-IFN treatment ALT and AFP levels are significantly associated with hepatocarcinogenesis [8], the influence of ALT and AFP levels after IFN treatment was determined in TT and nonTT patients to address possible reasons associated with higher HCC development observed in nonSVRs with rs8099917 nonTT. Overall, mean serum ALT and AFP levels were reduced after IFN therapy. However, the reduction observed in mean ALT and AFP levels after IFN therapy was less in nonTT patients than in TT patients among nonSVRs (Fig. 3). The cutoff values of ALT and AFP after IFN treatment for predicting patients without HCC developments were determined as ALT <40 IU/L and AFP <6.0 ng/mL by the receiver–operator characteristics curves analysis in the original cohort [8]. The cumulative incidence of HCC development in nonSVRs was less in patients whose post-IFN ALT or AFP levels were below these cutoff values (Fig. 4a, b). Even in patients whose ALT ≥40 IU/L or AFP ≥6.0 ng/mL before IFN therapy, patients with a reduction of ALT <40 IU/L or AFP <6.0 ng/mL after IFN therapy showed significantly lower cumulative development of HCC than those without reduction in both TT and nonTT subgroups (Fig. 4c–f). However, the proportion of patients with reduction of ALT <40 IU/L or AFP <6.0 ng/mL after IFN therapy in nonSVRs was significantly smaller in nonTT patients than TT patients (Fig. 5).

As reported in the recent study [8], the persistence of post-IFN treatment ALT or AFP levels to more than the cutoff values after IFN therapy was associated with a significantly higher incidence of HCC in both SVRs and nonSVRs (Supplementary Figure). In contrast, even in nonSVRs with an equal or higher pre-IFN treatment ALT or AFP level than the cutoff values, the cumulative incidence of HCC was significantly suppressed in patients whose post-IFN treatment ALT or AFP level was reduced to less than the cutoff values (Supplementary Figure).

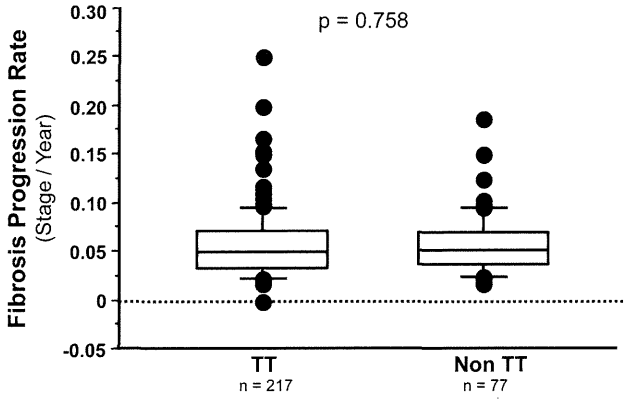

Fig. 2 Changes in fibrosis staging over time. Analysis in patients who showed evidence of a single blood transfusion as a known time of HCV infection ($n = 292$)

Influence of the SNPs near *IL28B* on HCC risk

Univariate analysis demonstrated that nonTT was one of the factors that increased the risk ratio for HCC development (Table 2). In the multivariate Cox model, age, sex, stage of fibrosis, pre-IFN treatment AFP level, post-IFN treatment ALT and AFP levels were independently associated with HCC risk among covariates including age, sex, stage of fibrosis, pre- and post-IFN treatment ALT and AFP levels, virological response and the SNPs near *IL28B* (Table 3). In patients infected with HCV genotype 1 who were treated with PEG-IFNα/RBV combination therapy, the SNPs near *IL28B* as well as age, sex, post-IFN treatment ALT level and pre-IFN treatment AFP level were identified as independent factors associated with the development of HCC among covariates including age, sex, stage of liver fibrosis, pre- and post-IFN treatment ALT and AFP levels, and virological response (Table 4). Although pre-IFN treatment AFP levels were significantly higher in patients with nonTT (Table 1; Fig. 3), our results for the multivariate analysis in this subgroup suggests that higher HCC incidence in nonTT patients is not fully explained by higher pre-IFN treatment AFP levels.

Discussion

By analyzing a large-scale, long-term cohort, we demonstrated that rs8099917 nonTT is significantly associated with HCC development particularly in patients infected with HCV genotype 1 who were treated with PEG-IFNα/RBV combination therapy. The possible relationship between the SNPs near *IL28B* and the risk of HCC development is controversial [11–13] mainly because of the lack of a longitudinal cohort study such as ours. Another possible reason for this controversy is the influence of antiviral therapy because the SNPs near *IL28B* are

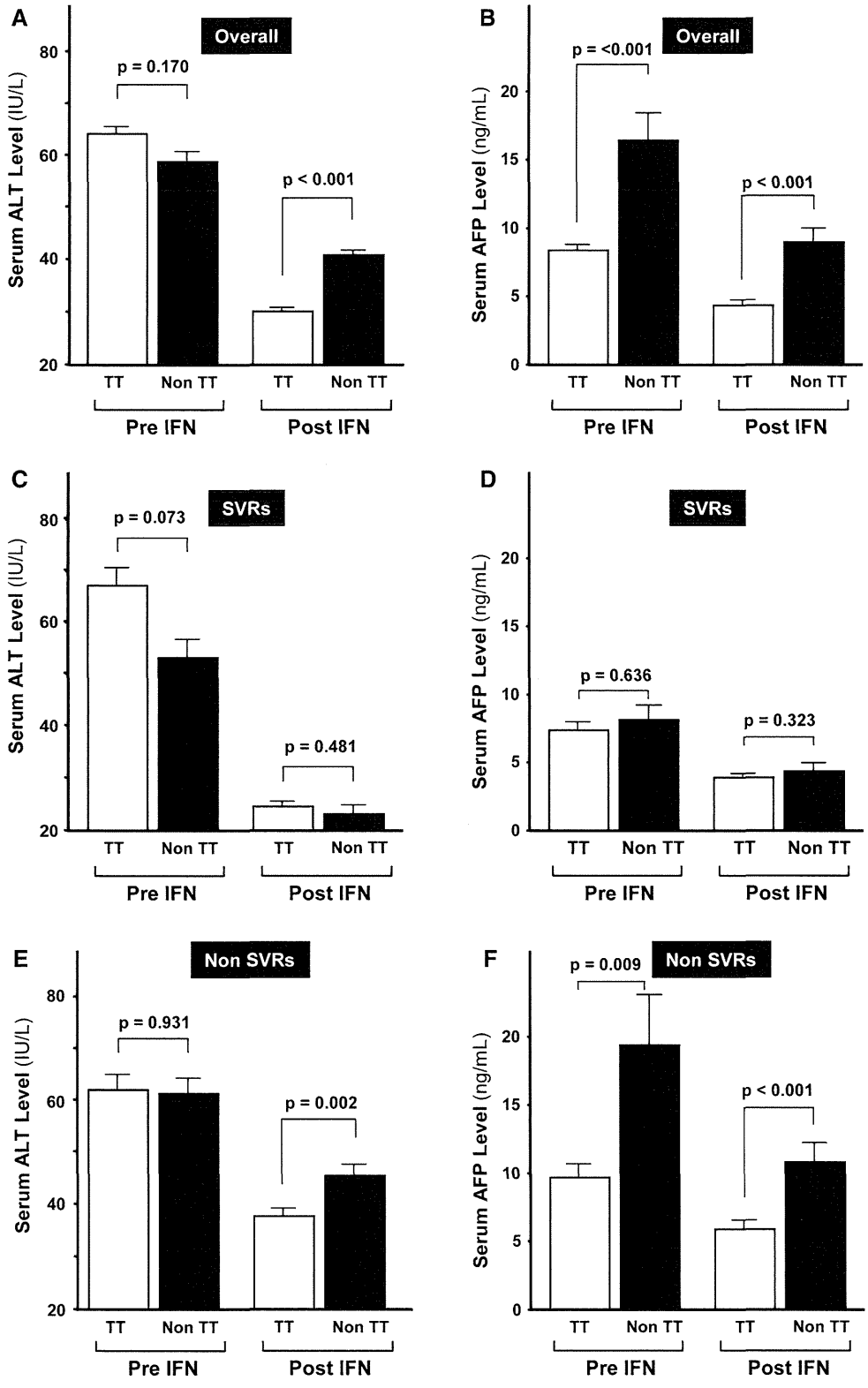

Fig. 3 Mean integration ALT and AFP values before and after interferon therapy in rs8099917 TT and nonTT patients. *Error bars* indicate the standard error. *p* values were determined by unpaired Student's *t* test

strongly associated with the antiviral response. Recent cross-sectional studies in patients without IFN treatment could not ascertain the relationship between the SNPs near *IL28B* and HCV-related HCC [12, 13]. From this viewpoint, our cohort is unique in that it includes only IFN-treated patients. In the Kaplan–Meier analyses, significantly higher incidence of HCC in nonTT was observed in patients infected with HCV genotype 1 and/or those treated with PEG-IFNα/RBV combination therapy, whereas it was not in patients infected with HCV genotype non-1 and

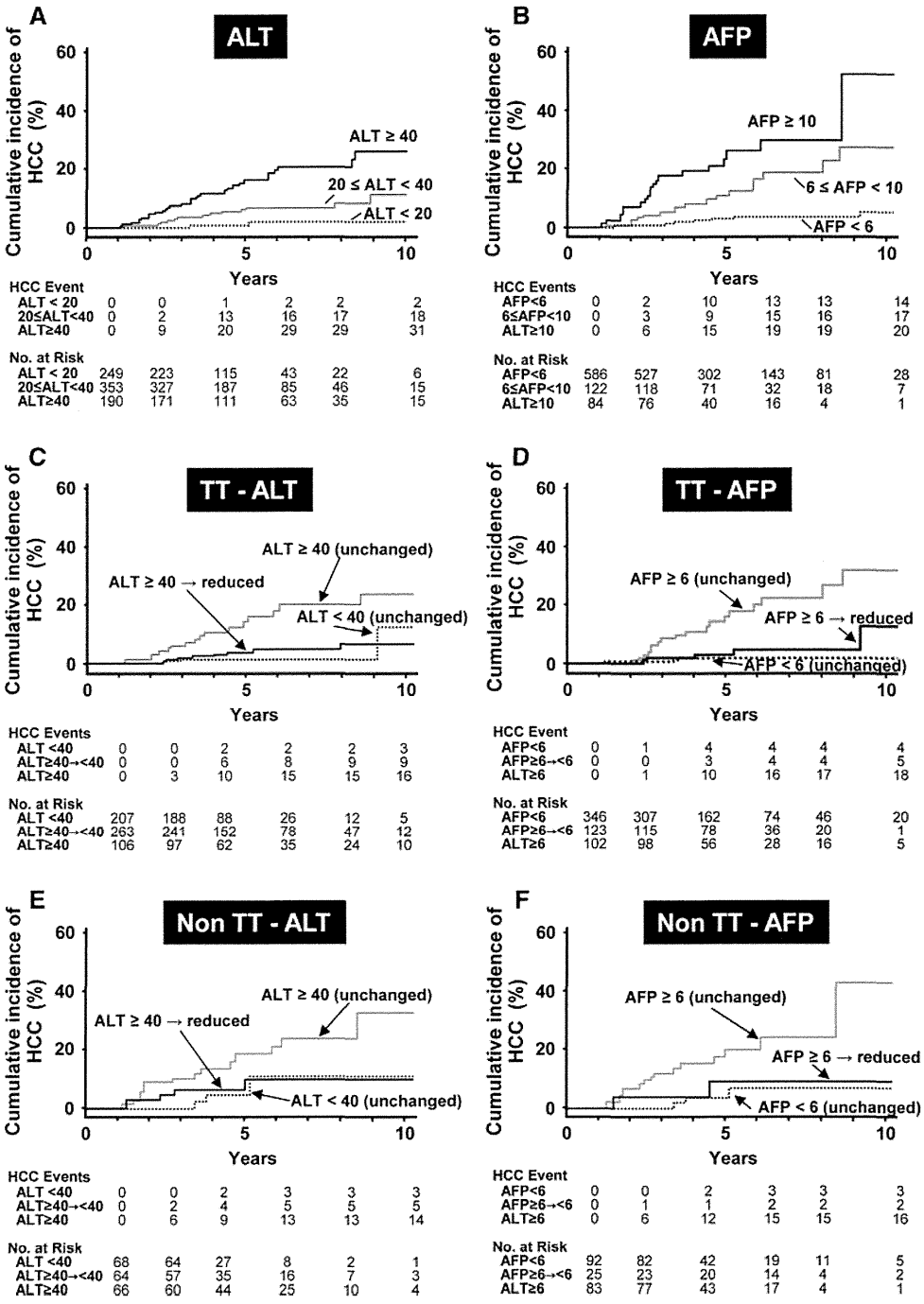

Fig. 4 Cumulative incidence of HCC stratified by mean integration values of post-IFN ALT and AFP levels. **a** Stratified by post-IFN treatment levels of ALT in all patients. Logrank test: $p < 0.001$. **b** Stratified by post-IFN treatment levels of AFP in all patients. Logrank test: $p < 0.001$. **c** According to changes in mean ALT levels before and after interferon therapy in patients with rs8099917 TT. Logrank test: $p < 0.001$. **d** According to changes in mean AFP levels before and after interferon therapy in patients with rs8099917 TT. Logrank test: $p < 0.001$. **e** According to changes in mean ALT levels before and after interferon therapy in patients with rs8099917 nonTT. Logrank test: $p = 0.040$. **f** According to changes in mean AFP levels before and after interferon therapy in patients with rs8099917 nonTT. Logrank test: $p < 0.001$

those treated other than PEG-IFNα/RBV. Moreover, our multivariate analyses demonstrated that an independent association between rs8099917 nonTT and HCC development was only found in patients infected with HCV genotype 1 who were treated with PEG-IFNα/RBV combination therapy. Because the SNPs near *IL28B* affects antiviral response particularly in patients infected with HCV genotype 1 and/or those treated with PEG-IFNα/RBV therapy, impact of the SNPs near *IL28B* on HCC risk may be indirect and is largely influenced by treatment effect.

Because a significantly higher incidence of HCC in nonTT patients was observed even in nonSVRs, higher HCC risk related to nonTT was not fully explained by the poor virological response rates observed in nonTT patients. Although we have reported that higher post-IFN treatment ALT and AFP levels were significantly associated with the risk of HCC [8], the relationship between *IL28B* SNPs and post-IFN treatment ALT and AFP levels has not yet been elucidated. Hence, to further address the higher HCC risk in nonTT patients, we directed our study at post-IFN

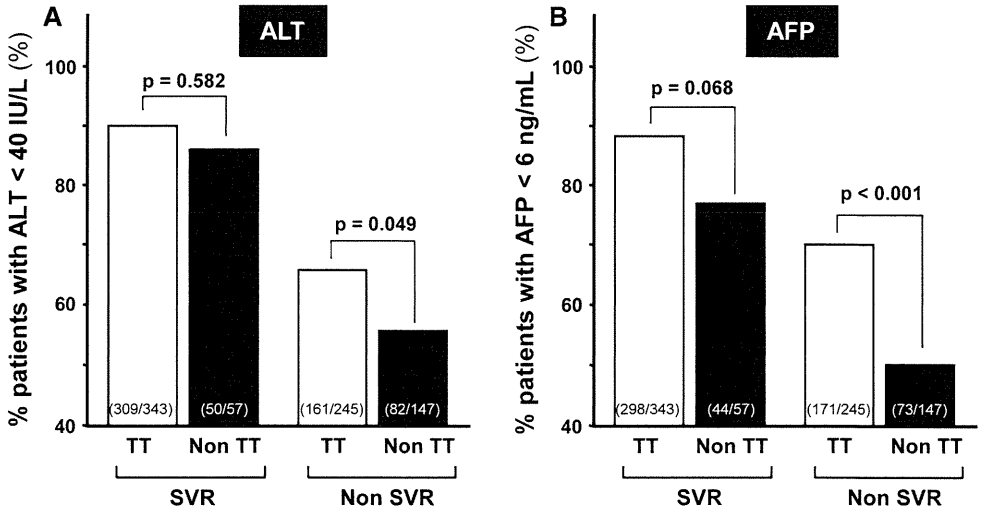

Fig. 5 Proportion of patients with reduction of ALT <40 IU/L or AFP <6.0 ng/mL after IFN therapy. **a** Percentage of patients with ALT <40 IU/L after IFN. **b** Percentage of patients with AFP <6 ng/mL after IFN

Table 2 Univariate analysis for the factors associated with hepatocellular carcinoma

Risk factor	Hazard ratio (95 % CI)	*p* value
IL28B genotype		
rs8099917 TT	1	
rs8099917 nonTT	2.36 (1.37–4.06)	0.002
Age (by every 10 year)	2.22 (1.51–3.28)	<0.001
Sex		
Female	1	
Male	2.17 (1.25–3.75)	0.006
Fibrosis stage		
F1/F2	1	
F3/F4	4.86 (2.82–8.37)	<0.001
γ-GTP (by every 40 IU/L)	1.27 (1.13–1.43)	<0.001
Core 70 mutation		
Wild	1	
Mutant	2.52 (0.94–6.78)	0.066
ISDR		
More than 1 mutation	1	
Wild or 1 mutation	1.08 (0.56–2.06)	0.826
IFN regimen		
IFN mono	1	
IFN + RBV	0.78 (0.31–1.98)	0.602
PEG-IFN mono	0.66 (0.27–1.61)	0.359
PEG-IFN + RBV	0.53 (0.25–1.12)	0.098
Pre-treatment ALT (by every 40 IU/L)	1.13 (1.00–1.22)	0.049
Post-treatment ALT (by every 40 IU/L)	3.02 (2.21–3.96)	<0.001
Pre-treatment AFP (by every 10 ng/mL)	1.09 (1.05–1.13)	<0.001
Post-treatment AFP (by every 10 ng/mL)	1.17 (1.09–1.26)	<0.001
Virological response		
SVR	1	
Non-SVR	3.07 (1.58–5.99)	0.001

Hazard ratios for the development of hepatocellular carcinoma were calculated by the Cox proportional hazards regression analysis

Table 3 Multivariate analysis for the factors associated with hepatocellular carcinoma in all patients

Risk factor	Hazard ratio (95 % CI)	*p* value
IL28B genotype		
rs8099917 TT	1	
rs8099917 nonTT	1.29 (0.72–2.33)	0.395
Age (by every 10 year)	2.59 (1.72–3.87)	<0.001
Sex		
Female	1	
Male	3.30 (1.80–6.06)	<0.001
Fibrosis stage		
F1/F2	1	
F3/F4	2.40 (1.36–4.24)	0.003
Pre-treatment ALT (by every 40 IU/L)	1.04 (0.89–1.17)	0.783
Post-treatment ALT (by every 40 IU/L)	2.58 (1.74–3.81)	<0.001
Pre-treatment AFP (by every 10 ng/mL)	1.38 (1.13–1.68)	0.002
Post-treatment AFP (by every 10 ng/mL)	1.61 (1.04–2.39)	0.028
Virological response		
SVR	1	
Non-SVR	1.64 (0.80–3.39)	0.177

Hazard ratios for the development of hepatocellular carcinoma were calculated by the Cox proportional hazards analysis

treatment ALT and AFP levels, which are considered to be possible biomarkers for the future development of HCC [8, 14]. These further analyses showed notable findings, which demonstrated that a decrease in ALT and AFP levels after IFN therapy is less in nonTT patients among nonSVRs, and

Table 4 Multivariate analysis for the factors associated with hepatocellular carcinoma in patients infected with HCV genotype 1 who were treated with PEG-IFNα/RBV combination therapy

Risk factor	Hazard ratio (95 % CI)	*p* value
IL28B genotype		
rs8099917 TT	1	
rs8099917 nonTT	4.50 (1.61–12.6)	0.004
Age (by every 10 year)	3.19 (1.72–5.99)	<0.001
Sex		
Female	1	
Male	6.17 (2.07–18.5)	0.001
Fibrosis stage		
F1/F2	1	
F3/F4	2.44 (0.86–6.97)	0.093
Pre-treatment ALT (by every 40 IU/L)	0.92 (0.59–1.49)	0.769
Post-treatment ALT (by every 40 IU/L)	2.38 (1.08–5.18)	0.034
Pre-treatment AFP (by every 10 ng/mL)	1.07 (1.01–1.13)	0.025
Post-treatment AFP (by every 10 ng/mL)	1.09 (0.94–1.27)	0.225
Virological response		
SVR	1	
Non-SVR	1.86 (0.46–7.41)	0.382

Hazard ratios for the development of hepatocellular carcinoma were calculated by the Cox proportional hazards analysis

that the proportions of patients with reductions of ALT <40 IU/L or AFP <6.0 ng/mL after IFN therapy in nonSVRs are significantly smaller in nonTT patients (Fig. 5). Although the essential mechanisms responsible for the relationship between elevated levels of ALT or AFP and HCC development are not known, these results suggest that a higher incidence of HCC observed in nonTT patients partly results from the limited suppressive effect of IFN on ALT and AFP levels, and might be reduced even in nonTT patients, whose ALT and/or AFP levels decrease after IFN-based antiviral treatment.

NonTT patients in our study exhibited a significant association with higher γ-glutamyl transpeptidase levels, increased frequency of hepatic steatosis, and increased frequency of the HCV core 70QH mutation; all these factors are associated with HCC development [2]. Therefore, HCC risk found in nonTT patients may also result from those factors coexisting with the *IL28B* minor allele.

Our results demonstrated that the SNPs near *IL28B* appeared to be independent of liver fibrosis. Recently, an association between the *IL28B* major allele and higher cirrhosis prevalence was reported in human immunodeficiency virus–HCV coinfected patients [15]. However, the limitations of this study were that it was a cross-sectional study involving only human immunodeficiency virus coinfected patients; moreover, hepatic elastography was used for determining liver fibrosis. Conversely, Marabita et al. [16] estimated the fibrosis progression rate in 247 patients with a known date of infection, and demonstrated that the *IL28B* genotype has no effect on the risk of developing advanced fibrosis. A recent study on the Swiss and the French cohorts showed a significant relationship between nonTT and a slow FPR; however, this relationship was found only in genotype non1-infected patients, and not in genotype 1-infected patients [17]. Our analysis of the FPR in HCV genotype 1b-dominant patient group demonstrated that the liver FPR did not differ between TT and nonTT patients. Taken together, the SNPs near *IL28B* do not appear to be closely associated with liver fibrogenesis in HCV genotype 1 monoinfected patients.

This study had a few limitations. The first was the heterogeneity of our cohort, which included various treatment regimens with different treatment responses. However, we obtained results in a more uniform subgroup of HCV genotype 1 patients treated with PEG-IFNα/RBV. The second limitation was the ethnic homogeneity of the Japanese population, who had a low minor allele frequency. A recent cross-sectional study in the Swiss cohort demonstrated a poor association between polymorphisms near *IL28B* and HCC occurrence [17]. Although many patients were included in that Swiss study, the number of patients with HCC development was few (3 %), which was inadequate to detect a significant effect of the polymorphism. Because the overall HCC risk varies among population groups (i.e. Japanese > European), longer-term longitudinal studies in larger cohorts with various population subgroups are required to verify the generality of our results. The third limitation involved the subanalyses of the original cohort. However, as shown in the Supplementary Table 1, SVR rates were equivalent between the original and the subcohort, although slight differences were found in proportion of gender, age and ALT levels. Moreover, characteristics of the patients with HCV genotype 1 who were treated with PEG-IFNα/RBV were identical between the original and the subcohort (Supplementary Table 2). Therefore, selection bias was unlikely to have affected our results, particularly in patients with HCV genotype 1 who were treated with PEG-IFNα/RBV, in whom SNPs near *IL28B* were identified as an independent factor associated with HCC development. The fourth limitation was that the effect of liver-supporting therapy such as ursodeoxycholic acid and glycyrrhizin was unclear in the present study, which may reduce ALT level and HCC risk in nonSVRs. However, it is likely that liver-supporting therapy was evenly indicated for both rs8099917 TT and nonTT patients, because we usually excluded the SNPs near *IL28B* from consideration when making decisions on therapeutic

indications of liver-supporting therapy. Moreover, suppressive effect on HCC development by liver-supporting therapy is presumably weak. Therefore, the effect of liver-supporting therapy was unlikely to have affected our results.

In conclusion, rs8099917 nonTT is a risk factor for HCC, in particular in patients infected with HCV genotype 1 who were treated with PEG-IFNα/RBV combination therapy. The effect of the SNPs near *IL28B* on HCC risk may be indirect, and higher HCC development observed in nonTT is presumably because of two reasons: (1) poor IFN efficacy in reducing ALT and/or AFP levels in patients with nonTT, (2) coexisting unfavorable risk factors for HCC. Not only HCV eradication but also suppression of ALT and/or AFP levels after IFN therapy may reduce the risk of hepatocarcinogenesis in nonTT patients.

Acknowledgments This study was supported by grants from the Japanese Ministry of Education, Culture, Sports, Science, and Technology and the Japanese Ministry of Health, Labor, and Welfare.

Conflict of interest Dr. Asahina received research funds from Daiichi-Sankyo and Chugai Pharma. Dr. Asahina and Dr. Kakinuma belong to a donation-funded department funded by Chugai Pharma, Toray, BMS, Dainippon-Sumitomo Pharma, and MSD.

References

1. Kiyosawa K, Sodeyama T, Tanaka E, Gibo Y, Yoshizawa K, Nakano Y, et al. Interrelationship of blood transfusion, non-A, non-B hepatitis and hepatocellular carcinoma: analysis by detection of antibody to hepatitis C virus. Hepatology. 1990;12:671–5.
2. Asahina Y, Tsuchiya K, Tamaki T, Hirayama I, Tanaka T, Sato M, et al. Effect of aging on risk for hepatocellular carcinoma in chronic hepatitis C virus infection. Hepatology. 2010;52:518–27.
3. Yoshida H, Shiratori Y, Moriyama M, Arakawa Y, Ide T, Sata M, et al. IFN therapy reduces the risk for hepatocellular carcinoma: national surveillance program of cirrhotic and noncirrhotic patients with chronic hepatitis C in Japan. Ann Intern Med. 1999;131:174–81.
4. Bruno S, Stroffolini T, Colombo M, Bollani S, Benvegnù L, Mazzella G, et al. SVR to IFN-alpha is associated with improved outcome in HCV-related cirrhosis: a retrospective study. Hepatology. 2007;45:579–87.
5. Tanaka Y, Nishida N, Sugiyama M, Kurosaki M, Matsuura K, Sakamoto N, et al. Genome-wide association of IL28B with response to pegylated IFN-alpha and ribavirin therapy for chronic hepatitis C. Nat Genet. 2009;10:1105–9.
6. Suppiah V, Moldovan M, Ahlenstiel G, Berg T, Weltman M, Abate ML, et al. IL28B is associated with response to chronic hepatitis C IFN-alpha and ribavirin therapy. Nat Genet. 2009;10:1100–4.
7. Ge D, Fellay J, Thompson AJ, Simon JS, Shianna KV, Urban TJ, et al. Genetic variation in IL28B predicts hepatitis C treatment-induced viral clearance. Nature. 2009;461:399–401.
8. Asahina Y, Tsuchiya K, Nishimura T, Muraoka M, Suzuki Y, Tamaki N, et al. α-fetoprotein levels after interferon therapy and risk of hepatocarcinogenesis in chronic hepatitis C. Hepatology. 2013. doi:10.1002/hep.26442.
9. Asahina Y, Tsuchiya K, Muraoka M, Tanaka K, Suzuki Y, Tamaki N, et al. Association of gene expression involving innate immunity and genetic variation in interleukin 28B with antiviral response. Hepatology. 2012;55:20–9.
10. Desmet VJ, Gerber M, Hoofnagle JH, Manns M, Scheuer PJ. Classification of chronic hepatitis: diagnosis, grading and staging. Hepatology. 1994;19:1513–20.
11. Eurich D, Boas-Knoop S, Bahra M, Neuhaus R, Somasundaram R, Neuhaus P, et al. Role of IL28B polymorphism in the development of hepatitis C virus-induced hepatocellular carcinoma, graft fibrosis, and posttransplant antiviral therapy. Transplantation. 2012;93:644–9.
12. Agúndez JA, García-Martin E, Maestro ML, Cuenca F, Martínez C, Ortega L, et al. Relation of IL28B gene polymorphism with biochemical and histological features in hepatitis C virus-induced liver disease. PLoS ONE. 2012;7:e37998.
13. Joshita S, Umemura T, Katsuyama Y, Ichikawa Y, Kimura T, Morita S, et al. Association of IL28B gene polymorphism with development of hepatocellular carcinoma in Japanese patients with chronic hepatitis C virus infection. Hum Immunol. 2012;73:298–300.
14. Osaki Y, Ueda Y, Marusawa H, Nakajima J, Kimura T, Kita R, et al. Decrease in alpha-fetoprotein levels predicts reduced incidence of hepatocellular carcinoma in patients with hepatitis C virus infection receiving interferon therapy: a single center study. J Gastroenterol. 2012;47:444–51.
15. Barreiro P, Pineda JA, Rallon N, Naggie S, Martín-Carbonero L, Neukam K, et al. Influence of interleukin-28B single-nucleotide polymorphisms on progression to liver cirrhosis in human immunodeficiency virus-hepatitis C virus-coinfected patients receiving antiretroviral therapy. J Infect Dis. 2011;203:1629–35.
16. Marabita F, Aghemo A, Nicola SD, Rumi MG, Cheroni C, Scavelli R, et al. Genetic variation in the interleukin-28B gene is not associated with fibrosis progression in patients with chronic hepatitis C and known date of infection. Hepatology. 2011;54:1127–34.
17. Bochud PY, Bibert S, Kutalik Z, Patin E, Guergnon J, Nalpas B, et al. IL28B alleles associated with poor HCV clearance protect against inflammation and fibrosis in patients infected with non-1 HCV genotypes. Hepatology. 2012;55:384–94.

Magn Reson Med Sci, Vol. 12, No. 2, pp. 77–86, 2013
doi:10.2463/mrms.2012-0052
©2013 Japanese Society for Magnetic Resonance in Medicine

MAJOR PAPER

MR-based Measurements of Portal Vein Flow and Liver Stiffness for Predicting Gastroesophageal Varices

Hiroyuki MORISAKA[1], Utaroh MOTOSUGI[1]*, Tomoaki ICHIKAWA[1], Katsuhiro SANO[1], Shintaro ICHIKAWA[1], Tsutomu ARAKI[1], and Nobuyuki ENOMOTO[2]

[1]*Department of Radiology and* [2]*First Department of Internal Medicine, University of Yamanashi*
1110 Shimokato, Chuo-shi, Yamanashi, Japan
(Received August 24, 2012; Accepted December 12, 2012; published online May 10, 2013)

Objectives: We evaluated flow parameters measured by phase-contrast magnetic resonance (MR) imaging (PC-MRI) of the portal venous system and liver stiffness measured by MR elastography (MRE) to determine the usefulness of these methods in predicting gastroesophageal varices (GEV) in patients with chronic liver disease (CLD).

Methods: In patients with CLD and controls, we performed PC-MRI on the portal (PV) and superior mesenteric veins; calculated mean velocity (V, cm/s), cross-sectional area (S, mm^2), and flow volume (Q, mL/min); and determined markers of liver fibrosis (liver stiffness [kPa]) and aspartate aminotransferase (AST) platelet ratio index [APRI]). We visually assessed GEV and development of collateral pathways of the PV on routine contrast-enhanced dynamic MR imaging and compared patient characteristics, flow parameters, liver stiffness markers, and visual analysis among 3GEV groups, those with mild, severe, or no GEV with reference to endoscopic findings.

Results: Child-Pugh grade, V_{PV}, S_{PV}, liver stiffness, APRI, and visually identified GEV (visible GEV) differed significantly among the 3 groups ($P<0.05$). We investigated V_{PV}, S_{PV}, liver stiffness, and visible GEV as independent markers to distinguish patients with and without GEV and examined V_{PV} and visible GEV to predict severe GEV. Visible GEV showed low sensitivity (14 to 30%) and high specificity (98%) for predicting GEV in patients with CLD. A subgroup analysis that excluded cases with collateral pathway demonstrated slightly improved diagnostic performance of V_{PV} and liver stiffness.

Conclusions: Portal vein flow parameters and liver stiffness can be useful markers for predicting GEV in patients with CLD.

Keywords: ***gastroesophageal varices, MR elastography, phase-contrast MRI***

Introduction

Gastroesophageal varices (GEV) and bleeding from them are severe complications of portal hypertension in patients with chronic liver disease (CLD). GEV develop in 7% of patients with cirrhosis each year, and occurrence of a first variceal hemorrhage at one year from diagnosis is approximately 12%.[1] Mortality associated with GEV bleeding ranges from 30 to 70%.[2] Combined treatments, such as vasoactive drugs (beta-blockers), endoscopic ligation, and transjugular intrahepatic portosystemic shunt, have been developed to prevent GEV bleeding.[3,4]

Liver fibrosis, a cause of portal hypertension, plays a fundamental role in the development of GEV, and clinicians must monitor patients with liver fibrosis for them. Endoscopy is commonly used to identify GEV, but screening is time consuming and costly, and serious complications, though rare, can occur. Ideally, endoscopic screening for GEV would be restricted to a well targeted population of patients with cirrhosis.

Phase-contrast MR imaging (PC-MRI) has been developed in many fields to measure flow in the

*Corresponding author, Phone: +81-55-273-1111, Fax: +81-55-273-6744, E-mail: utaroh-motosugi@nifty.com

cardiovascular system, pulmonary artery, cerebrospinal fluid, and portal venous system.[5-8] Liver cirrhosis and portal hypertension change the hemodynamics of the portal venous system.[9] Demonstration by a previous study of altered rate of flow in the portal vein (PV) in patients with GEV suggested that flow in the vessel might serve as a predictor of GEV bleeding.[10]

Patients with high risk of developing GEV can also be targeted by estimating degree of liver fibrosis using recently developed methods or a clinically useful blood biochemical index, such as aspartate aminotransferase (AST) platelet ratio index (APRI).[11-15] MR elastography (MRE) is a state-of-the-art tool for evaluating liver stiffness that offers high reproducibility, repeatability, and validity.[16-21]

MR examination of the liver can be shortened by performing both PC-MRI and MRE during the delay before equilibrium- or hepatocyte-phase after administration of a contrast agent.[22,23] Use of these examinations to predict GEV would significantly enhance the utility of MR imaging in managing patients with cirrhosis.

We evaluated the utility of flow parameters measured by PC-MRI of the portal venous system and liver stiffness measured by MRE of the liver for predicting GEV in patients with CLD.

Materials and Methods

Subjects

Our institutional review board approved this retrospective study, and written informed consent was waived. March 1 through December 31 in 2011, 697 patients underwent both PC-MRI of the portal venous system (PV) and superior mesenteric vein (SMV) and MRE at our institution; 305 of the 697 had CLD. We randomly selected 60 control subjects from the patients without CLD who exhibited no liver abnormality other than hepatic cyst or hemangioma, which was confirmed by clinical follow-up and multi-imaging modalities. Of the 305 patients with CLD, we excluded 110 patients who met at least one of the following 5 criteria: 64 patients who did not undergo upper endoscopic examination within 6 months of MR examination; 28 with history of interventional treatment for GEV, such as endoscopic ligation and balloon-occluded retrograde transvenous obliteration; five with PV thrombus confirmed by contrast-enhanced computed tomography; four for whom PC-MRI failed because of motion artifact; and nine with history of lobectomy or more than one segmentectomy of the liver. This yielded a study cohort of 195 patients with CLD who underwent at least one upper endoscopic examination within 6 months of PC-MRI (Fig. 1).

CLD types included 130 cases positive for hepati-

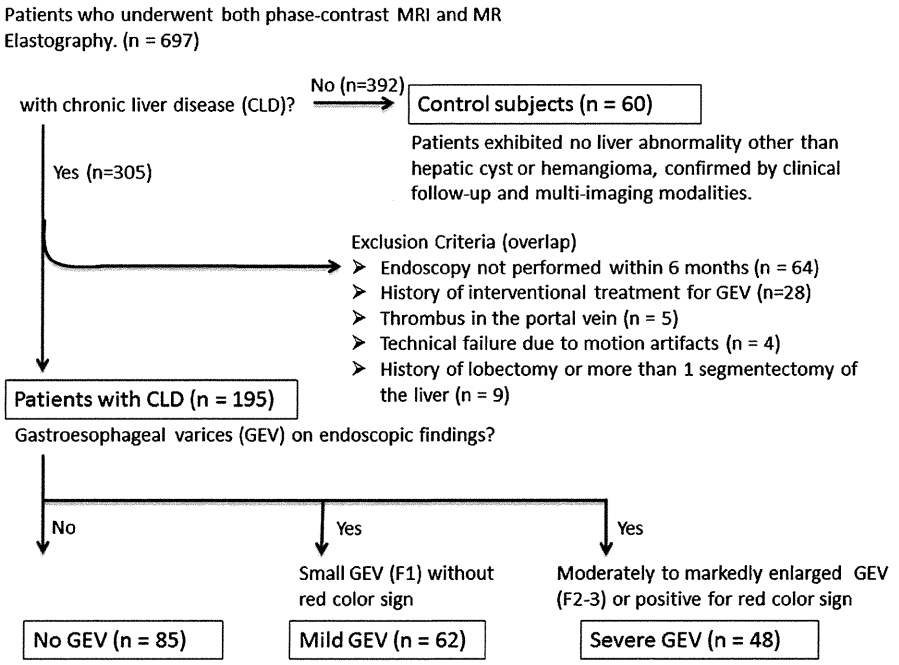

Fig. 1. Schematic diagram of inclusion/exclusion criteria and selection process of study cohort.

tis C virus, 27 positive for hepatitis B virus, 17 with alcoholic liver disease, three with autoimmune liver disease, and 18 other types. Characteristics of controls were: age, 63 ± 13 years; body weight, 54 ± 9 kg; and male-to-female ratio, 40/20. Characteristics of the CLD group were: age, 69 ± 9 years; body weight, 59 ± 10 kg; and male-to-female ratio, 118/75. These characteristics did not differ significantly between the control and study subjects.

Reference standard of GEV

Gastroenterologists specialized in endoscopy from our institution's Department of Digestive Medicine performed all upper endoscopic examinations, recording the presence or absence of GEV. When GEV was present, they identified the form of GEV and type of red color (RC) sign, according to the general rules for recording endoscopic findings of esophagogastric varices (Second Edition of the Japanese Research Society for Portal Hypertension).[24] This system categorizes forms of varices as: straight and small, F1; moderately enlarged and beady, F2; markedly enlarged and nodular or tumor-shaped, F3. Results of endoscopic examinations of patients with history of GEV bleeding within 6 months of PC-MRI were designated positive for RC sign regardless of other endoscopic findings.

We divided patients into 3 groups by GEV form and RC sign on endoscopic findings: 85 patients with no GEV (Fig. 2a); 62 patients with mild GEV, with F1 and negative RC sign (Fig. 2b); and 48 patients with severe GEV, with either F2–F3 or positive RC sign (Fig. 2c). We recommended endoscopic treatment in our institution for patients with severe GEV (Fig. 2c).

PC-MRI

To avoid confounding effect of increased mesenteric blood flow from eating,[25,26] all subjects fasted at least 3 hours before undergoing MR imaging examination using a 1.5-tesla scanner (Signa; GE Healthcare, Milwaukee, WI, USA). For reference, we acquired images of 4-mm thick coronal slices of the portal venous system using FIESTA sequence (fast imaging employing steady-state acquisition). All patients underwent breath-hold 2-dimensional (2D) PC-MRI to measure flow in the PV and SMV. Slices were set as cross-sections perpendicular to the direction of flow of the PV and SMV (Fig. 3). Imaging parameters for PC-MRI were: repetition time (TR)/echo time (TE), 12.5/5 ms; flip angle,

Fig. 2. Representative endoscopic findings of gastroesophageal varices (GEV). **(a)** None, **(b)** mild, and **(c)** severe.

Fig. 3. Left, reference coronal steady-state acquisition images (FIESTA) of the portal venous system. White lines represent cross-sections perpendicular to flow direction of the portal and superior mesenteric veins. Right, magnitude images of phase-contrast magnetic resonance (MR) imaging of corresponding cross-sections with circular regions of interest placed on each vein.

Table 1. Magnetic resonance imaging parameters

Parameters	Phase-contrast MR imaging	MR elastography
Sequence	Gradient echo	Gradient echo
TR/TE (ms)	12.5/5.0	100/27
Flip angle	20°	30°
Slice thickness (mm)	10	10
Field of view (cm)	40×28	30 to 34×40 to 45
Matrix	256×128	256×64
Number of slices	2*	2
Others	Velocity encoding parallel to flow direction: 30 cm/s	Frequency of pneumatic driver: 60 Hz

MR, magnetic resonance; TE, echo time; TR, repetition time; * One slice each for portal vein and superior mesenteric vein was applied.

20°; slice thickness, 10 mm; FOV, 40×28 cm; matrix, 256×126; number of slices, one; number of phases, 30; velocity encoding parallel to flow direction, 30 cm/s (Table 1). During PC-MRI, peripheral arterial pulses were monitored on the fingertip and synchronized to the pulse sequence of the MR imaging.

A radiologist with 7 years' experience in abdomi-

nal radiology selected a region of interest (ROI) on each vein in which to measure mean velocity (V, cm/s), area (S, mm^2), and flow volume (Q, mL/min) of the PV and SMV. The ROI placed on the magnitude image first was copied onto the phase image. We calculated flow-related parameters using Advantage Workstation software (GE Healthcare). Because flow velocity fluctuates during the cardiac cycle in the portal venous system, we calculated flow volume by integrating flow volume during a cardiac cycle and then multiplying that value by the number of heartbeats.

Visual analysis

We visually assessed routine dynamic contrast-enhanced MR imaging in all patients for the presence or absence of GEV (visible GEV), defined as luminal dilated vessels abutting or protruding into the luminal space,[27] and visible collateral pathways of the PV, defined as tortuously dilated paraumbilical vein, spleno-renal shunt, and paraesophageal vein.

MR elastography

MRE was performed by attaching a cylindrical passive driver across the patient's right chest wall using an elastic (rubber) belt to deliver a pneumatic vibration to the chest wall and liver via a plastic cylinder from a generator placed outside the MR examination room. The generator of the vibration and passive driver were developed at the Mayo Clinic (Rochester, MN, USA).

We employed a breath-hold 2D gradient-echo MRE sequence to acquire axial wave images, setting the scanning position above the gallbladder and below the subphrenic region of the liver.[14] MRE imaging parameters were: (TR/TE), 100/27 ms; continuous sinusoidal vibration, 60 Hz; FOV, 30 to 34 cm × 40 to 45 cm; matrix size, 256 × 64; flip angle, 30°; slice thickness, 10 mm; number of slices, 2; evenly spaced phase offsets, 4; and a single cycle of a 60-Hz trapezoidal motion-encoding gradient, with zero- and first-moment nulling along the through-plane direction. We did not use parallel imaging. Total acquisition time was 64 s (four 16-s breath holds) (Table 1). The MR scanner automatically generated elastograms by processing the acquired propagating shear wave images using a previously described inversion algorithm. Shear stiffness of the tissue was determined as a pixel value (kPa).

We evaluated the ROI in the right lobe of the liver on the elastogram in the slice proximal to the center of the passive driver placed on the patient's chest wall. We did not use the left lobe for ROI measurement to avoid the effects of cardiac motion on the MRE phase image. Generally, we placed ROIs of 1.0 to 1.5 cm^2 near the anterior edge of the liver where the penetrating wave was well visualized and no interference was observed on the phase image. The magnitude image was also used to place the ROI in the liver region to avoid intrahepatic vessels or bile ducts. The average value in the ROI was used as an indicator of liver stiffness by MRE.

Blood test-based hepatic fibrosis marker

As a blood test-based marker of liver fibrosis, we used AST platelet ratio index (APRI), calculated as[28]: APRI = (AST level/upper limit of AST)/(platelet counts/10^6) × 100. We consider the upper limit of AST as 32 IU/L at our institution.

Statistical analysis

We used Mann–Whitney *U* test to compare flow-related parameters by PC-MRI between patients with CLD and control subjects and Kruskal–Wallis test to assess univariate analysis of patients' characteristics (age, sex, body weight, and Child-Pugh grade), flow-related parameters, liver stiffness by MRE, and APRI among the 3 GEV groups. We then compared these findings with the proportions of visible GEV among the 3 GEV groups.

We used logistic regression to perform multivariate analyses to discriminate presence and absence of GEV and severe GEV from absent to mild GEV and included only the variables showing significant differences in the univariate analysis. Before multivariate analyses, we calculated a correlation coefficient between the variables to assess colinearity. We performed receiver operating characteristic (ROC) analysis to estimate the efficacy of discrimination. We also performed subgroup analysis that excluded patients with collateral pathways. All statistical analyses were performed using JMP version 9 software (SAS Institute Japan, Tokyo, Japan). Data are presented as mean ± standard deviation.

Results

Comparison of parameters by PC-MRI between patients with and without CLD

We observed statistically significant differences in V_{PV}, V_{SMV}, S_{PV}, S_{SMV} and Q_{SMV} between patients with CLD and control subjects (Table 2).

Comparison of parameters by PC-MRI and liver stiffness by MRE in patients with CLD

We observed statistically significant differences in Child-Pugh class, V_{PV}, S_{PV}, liver stiffness, APRI,

and distribution of visible GEV among the GEV groups (Table 3).

Multivariate analysis for discriminating presence or absence of GEV

None of the parameters showing significant differences in the univariate analyses (Child-Pugh grade, V_{PV}, S_{PV}, liver stiffness, APRI, and visible GEV) showed a square of correlation coefficient greater than 0.5; therefore, we included all these parameters in our multivariate analyses.

Multivariate regression analysis identified V_{PV}, S_{PV}, liver stiffness, and visible GEV as independent indicators for discriminating absence, presence, and degree of GEV (Table 4). The area under the ROC curve (AUC) was 0.70 for V_{PV}, 0.64 for S_{PV}, and 0.69 for liver stiffness. Visible GEV showed 14% sensitivity and 98% specificity. In a subgroup analysis that excluded 32 patients with collateral pathways, the diagnostic performances of V_{PV} and liver stiffness were slightly improved (Table 5); the AUC was 0.73 for V_{PV} and 0.71 for liver stiffness.

Multivariate analysis for discriminating severe from absent to mild GEV

Multivariate analysis demonstrated V_{PV}, S_{PV}, and visible GEV, but not liver stiffness, as independent indicators for discriminating severe from absent to mild GEV (Table 4). The AUC was 0.72 for V_{PV} and 0.64 for S_{PV}. Visible GEV showed 30% sensitivity and 98% specificity. In the subgroup analysis, the diagnostic performances of V_{PV} and S_{PV} did not change (Table 5). Figure 4 shows MR

Table 2. Comparison of parameters measured by phase-contrast magnetic resonance (MR) imaging between patients with and without chronic liver disease (CLD)

Flow measurement parameter	Control subjects n=60	Patients with CLD n=195	*P*-value
V_{PV} (cm/s)	12.3±3.0	8.5±2.7	<0.0001
S_{PV} (mm²)	106±35	141±50	0.002
Q_{PV} (mL/s)	734±207	713±298	0.33
V_{SMV} (cm/s)	7.4±2.6	6.5±2.4	0.029
S_{SMV} (mm²)	59±23	88±39	0.001
Q_{SMV} (mL/s)	261±126	336±186	0.03

Values are expressed as mean±standard deviation. CLD, chronic liver disease; PV, portal vein; Q, flow volume; S, cross-sectional area; SMV, superior mesenteric vein; V, mean velocity.

Table 3. Comparison of clinical characteristics and measured parameters among the 3 groups with no, mild, and severe gastroesophageal varices (GEV)

Variables	No GEV n=85	Mild GEV n=62	Severe GEV n=48	*P*-value
Age (years)	70±10	69±9	71±8	0.72
Male : Female	58 : 27	34 : 28	27 : 21	0.19
Body weight (kg)	59±11	57±12	57±18	0.45
Child-Pugh A/B/C	67/18/0	47/13/2	27/20/1	0.03
PC-MRI				
V_{PV} (cm/s)	10±3.0	8.1±2.1	7.1±2.0	<0.001
S_{PV} (mm²)	127±34	146±54	163±58	0.001
Q_{PV} (mL/s)	722±260	718±325	690±331	0.63
V_{SMV} (cm/s)	7.0±2.0	6.1±1.9	6.5±3.4	0.24
S_{SMV} (mm²)	80±32	98±46	88±37	0.11
Q_{SMV} (mL/s)	314±132	373±239	327±180	0.72
MRE				
Liver stiffness (kPa)	4.2±1.6	5.4±2.0	5.7±1.6	<0.001
APRI	1.8±2.0	1.6±1.5	2.4±1.3	<0.001
Visual analysis				<0.001
Visible GEV positive	1	1	14	
Visible GEV negative	84	60	33	

Values are expressed as mean±standard deviation. APRI, aspartate aminotransferase (AST) platelet ratio index ([AST level/32]/[platelet counts/10^6]×100); PV, portal vein; Q, flow volume; S, cross-sectional area; SMV, superior mesenteric vein; V, mean velocity.

Table 4. Multivariate analyses for discrimination of presence or absence of gastroesophageal varices (GEV) and severe from absent to mild GEV

Variate	Discrimination of presence of GEV from no GEV			Discrimination of severe GEV from no to mild GEV		
	OR	95%CI	*P*-value	OR	95%CI	*P*-value
V_{PV}	0.72	0.61–0.84	<0.001	0.69	0.56–0.83	0.001
Liver stiffness*	1.43	1.15–1.82	0.001	1.20	0.95–1.53	0.11
S_{PV}	11.7	1.4–123	0.03	1.00	0.99–1.01	0.09
APRI	0.37	0.03–3.6	0.39	1.18	0.90–1.51	0.41
Child-Pugh grade (B or C)	1.22	0.50–3.05	0.43	2.53	0.95–6.92	0.07
Visual analysis	19.7	2.7–435	0.001	60.1	11.6–543	<0.001

APRI, aspartate aminotransferase (AST) platelet ratio index ([AST level/32]/[platelet counts/10^6] × 100); CI, confidence interval; OR, Odds Ratio; PV, portal vein; S, cross-sectional area; V, mean velocity. * Liver stiffness was calculated by magnetic resonance (MR) elastography.

Table 5. Subgroup analyses of patients without visible collateral pathways for discrimination of presence or absence of gastroesophageal varices (GEV) and severe GEV from absent to mild GEV

Variate	Discrimination of presence and absence of GEV			Discrimination of severe GEV from no to mild GEV		
	OR	95%CI	p-Value	OR	95%CI	p-Value
V_{PV}	0.75	0.61–0.89	0.001	0.73	0.56–0.91	0.005
Liver stiffness	1.56	1.19–2.08	<0.001	1.09	0.78–1.49	0.920
S_{PV}	1.02	1.00–1.03	0.002	1.01	1.00–1.02	0.016
APRI	0.91	0.67–1.18	0.492	1.31	0.97–1.74	0.763
Child-Pugh grade (B or C)	0.59	0.18–1.78	0.512	1.62	0.48–5.43	0.557
Visual analysis	28.9	4.16–614	0.001	62.9	11.4–611	<0.001

APRI, aspartate aminotransferase (AST) platelet ratio index ([AST level/32]/[platelet counts/10^6] × 100); CI, confidence interval; OR, Odds Ratio; PV, portal vein; S, cross-sectional area; V, mean velocity.

elastograms, liver stiffness, and V_{PV} of representative cases from the 3 GEV groups (Fig. 4a, absent GEV; 4b, mild GEV; 4c, severe GEV).

Discussion

In this study, we sought to develop a noninvasive predictor of GEV using functional MR imaging. Some reports have suggested that PV flow volume calculated by PC-MRI or by Doppler ultrasound is not a useful predictor of advanced GEV,[27,29] and our data confirmed this. PV flow volume did not differ significantly between patients with CLD and controls. S_{PV} increased in proportion to the portal pressure in patients with GEV. As a result, measuring V_{PV} is more reliable than calculating PV flow volume for predicting GEV or portal hypertension, as shown in our analysis. We also demonstrated liver stiffness measured by MRE as a significant indicator for discriminating patients with and without GEV. However, though liver stiffness and APRI are valid markers of hepatic fibrosis, they were not useful predictors of clinically important or severe GEV. These results suggest that hepatic fibrosis develops before portal pressure increases.

In the subgroup analysis that excluded patients with collateral pathways of the portal venous system, the diagnostic performance of V_{PV} and liver stiffness were slightly improved. This result suggests that confounding factors of collateral pathway development negatively affect the diagnostic performance of these functional parameters.

Visibility of GEV on routine dynamic contrast-enhanced MR imaging showed high specificity (98%) and low sensitivity (14 to 30%) for predicting presence of GEV in this study; on routine MR imaging, only advanced dilated GEV was visibly identifiable. One previous report demonstrated moderate sensitivity (60–90%) and excellent specificity (70–100%) of computed tomography (CT) and MR imaging for detecting varices.[30] The different diagnostic criteria for varices of the previous

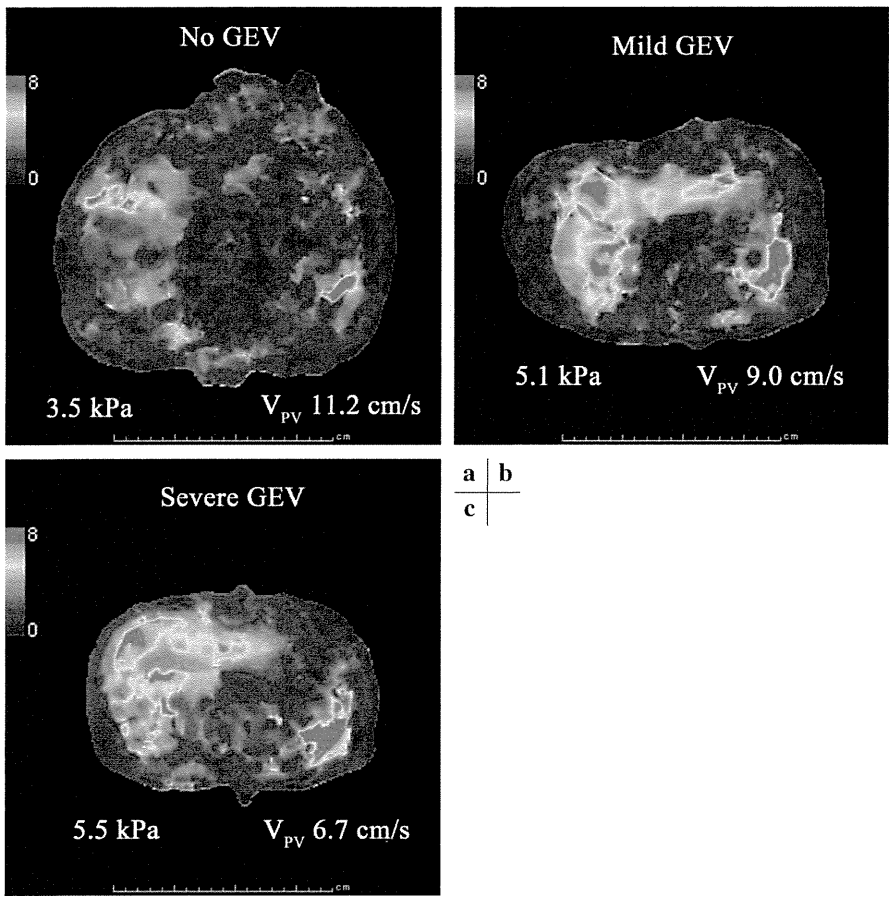

Fig. 4. Magnetic resonance (MR) elastogram, liver stiffness, and mean velocity of portal vein (V_{PV}) in representative cases of gastroesophageal varices (GEV), (**a**) absent, (**b**) mild, and (**c**) severe. (**a**) In a case without GEV, liver stiffness is not elevated and V_{PV} is not decreased. (**b**) In a mild case of GEV, liver stiffness is elevated and V_{PV} is mildly decreased. (**c**) In a severe case of GEV, liver stiffness is elevated and V_{PV} is significantly decreased.

report and ours may account for this discrepancy in sensitivity. Another more accurate morphological assessment of the portal venous system, such as 3D contrast-enhanced MR portography,[31] is also reported. However, we believe functional quantitative parameters may be more subjective than qualitative morphological assessment.

Previous Doppler ultrasound-based studies have found no significant difference in V_{PV} among variceal grades (e.g., small vs. large varices or F1 vs. F2 vs. F3 varices).[29,32] We speculate this discrepant finding is due to the different precision of the 2 measurement modalities. Doppler ultrasound can measure flow in the PV and may be cheaper and more widely available than PC-MRI. However, flow measurement is more valid by PC-MRI than ultrasonography, which yields more variable and overestimated results.[33]

The decreased V_{PV} in patients with GEV is thought to result from the constant rather than pulsatile flow of the venous system because the pressure gradient between the PV and the sinusoids of the liver is considered a driving force of PV flow. If sinusoidal pressure increases as hepatic fibrosis develops, the pressure gradient and V_{PV} will decrease. Thus, we propose a decrease in V_{PV} as a direct indicator of portal hypertension. Evaluating chronic pulmonary arterial hypertension (PAH) using breath-hold 2D cine PC-MRI applied to the pulmonary artery, Sanz and colleagues showed average pulmonary artery velocity to be the most useful parameter in predicting chronic PAH.[8] We speculate that a similar relationship exists between portal hypertension and V_{PV}.

Our study has some limitations. First, we did not assess the predictability of GEV bleeding, the most important clinical outcome. Further longitudinal evaluation is warranted; we hope functional MR imaging parameters may be more useful than morphological assessments in predicting future GEV

bleeding and clinical prognosis in patients with CLD. Second, it seemed we could eliminate the confounding effects of increased mesenteric venous flow from eating by having patients fast for at least 3 hours; the robustness of PV flow measurement on only one slice at a specific time point should be considered. Recently developed time-resolved 3- or 4-dimensional PC-MRI may soon resolve this problem.[34-36] The retrospective design also limited our study. We expect a prospective study with longitudinal observations would strengthen the conclusions of our study.

In conclusion, PV flow parameters measured by PC-MRI of the portal venous system and liver stiffness measured by MRE can be useful for identifying GEV in patients with CLD.

Acknowledgements

We would like to thank Richard Ehman of Mayo Clinic for providing MRE equipment, the gastroenterologists of our Department of Digestive Medicine for performing upper endoscopies and providing their findings, Satoshi Ikenaga and Hiroshi Kumagai, radiation technologists of our institute, and the other radiologists from our department for supporting us in MR examinations.

References

1. Garcia-Tsao G, Bosch J. Management of varices and variceal hemorrhage in cirrhosis. New Engl J Med 2010; 362:823-832.
2. Sarin SK, Lamba GS, Kumar M, Misra A, Murthy NS. Comparison of endoscopic ligation and propranolol for the primary prevention of variceal bleeding. New Engl J Med 1999; 340:988-993.
3. García-Pagán JC, Caca K, Bureau C, et al. Early use of TIPS in patients with cirrhosis and variceal bleeding. New Engl J Med 2010; 362:2370-2379.
4. Groszmann RJ, Garcia-Tsao G, Bosch J, et al. Beta-blockers to prevent gastroesophageal varices in patients with cirrhosis. New Engl J Med 2005; 353:2254-2261.
5. Applegate GR, Thaete FL, Meyers SP, et al. Blood flow in the portal vein: velocity quantitation with phase-contrast MR angiography. Radiology 1993; 187:253-256.
6. Stivaros SM, Sinclair D, Bromiley PA, Kim J, Thorne J, Jackson A. Endoscopic third ventriculostomy: predicting outcome with phase-contrast MR imaging. Radiology 2009; 252:825-832.
7. Wang ZJ, Reddy GP, Gotway MB, Yeh BM, Higgins CB. Cardiovascular shunts: MR imaging evaluation. Radiographics 2003; 23 Spec No:S181-S194.
8. Sanz J, Kuschnir P, Rius T, et al. Pulmonary arterial hypertension: noninvasive detection with phase-contrast MR imaging. Radiology 2007; 243: 70-79.
9. Liu H, Cao H, Wu ZY. Magnetic resonance angiography in the management of patients with portal hypertension. Hepatobiliary Pancreat Dis Int 2005; 4:239-243.
10. Burkart DJ, Johnson CD, Ehman RL, Weaver AL, Ilstrup DM. Evaluation of portal venous hypertension with cine phase-contrast MR flow measurements: high association of hyperdynamic portal flow with variceal hemorrhage. Radiology 1993; 188:643-648.
11. Castéra L, Vergniol J, Foucher J, et al. Prospective comparison of transient elastography, Fibrotest, APRI, and liver biopsy for the assessment of fibrosis in chronic hepatitis C. Gastroenterology 2005; 128:343-350.
12. Loaeza-del-Castillo A, Paz-Pineda F, Oviedo-Cárdenas E, Sánchez-Avila F, Vargas-Voráckova F. AST to platelet ratio index (APRI) for the noninvasive evaluation of liver fibrosis. Ann Hepatol 2008; 7:350-357.
13. Yin M, Talwalkar JA, Glaser KJ, et al. Assessment of hepatic fibrosis with magnetic resonance elastography. Clin Gastroenterol Hepatol 2007; 5:1207-1213.e2.
14. Motosugi U, Ichikawa T, Sano K, et al. Magnetic resonance elastography of the liver: preliminary results and estimation of inter-rater reliability. Jap J Radiol 2010; 28:623-627.
15. Huwart L, Sempoux C, Salameh N, et al. Liver fibrosis: noninvasive assessment with MR elastography versus aspartate aminotransferase-to-platelet ratio index. Radiology 2007; 245:458-466.
16. Huwart L, Sempoux C, Vicaut E, et al. Magnetic resonance elastography for the noninvasive staging of liver fibrosis. Gastroenterology 2008; 135:32-40.
17. Hines CD, Bley TA, Lindstrom MJ, Reeder SB. Repeatability of magnetic resonance elastography for quantification of hepatic stiffness. J Magn Reson Imaging 2010; 31:725-731.
18. Shire NJ, Yin M, Chen J, et al. Test-retest repeatability of MR elastography for noninvasive liver fibrosis assessment in hepatitis C. J Magn Reson Imaging 2011; 34:947-955.
19. Kim BH, Lee JM, Lee YJ, et al. MR elastography for noninvasive assessment of hepatic fibrosis: experience from a tertiary center in Asia. J Magn Reson Imaging 2011; 34:1110-1116.
20. Asbach P, Klatt D, Schlosser B, et al. Viscoelasticity-based staging of hepatic fibrosis with multifrequency MR elastography. Radiology 2010; 257:80-86.
21. Motosugi U, Ichikawa T, Sano K, et al. Magnetic resonance elastography of the liver: preliminary results and estimation of interrater reliability. Jpn J Radiol 2010; 28:623-627.

22. Motosugi U, Ichikawa T, Sou H, et al. Effects of gadoxetic acid on liver elasticity measurement by using magnetic resonance elastography. Magn Reson Imaging 2012; 30:128–132.
23. Yoshikawa T, Ohno Y, Motohara T, et al. Gadolinium-enhanced phase-contrast magnetic resonance portography. Magn Reson Med Sci 2005; 4:165–174.
24. Tajiri T, Yoshida H, Obara K, et al. General rules for recording endoscopic findings of esophagogastric varices (2nd edition). Dig Endosc 2010; 22:1–9.
25. Burkart DJ, Johnson CD, Reading CC, Ehman RL. MR measurements of mesenteric venous flow: prospective evaluation in healthy volunteers and patients with suspected chronic mesenteric ischemia. Radiology 1995; 194:801–806.
26. Tsukuda T, Ito K, Koike S, et al. Pre- and postprandial alterations of portal venous flow: evaluation with single breath-hold three-dimensional half-Fourier fast spin-echo MR imaging and a selective inversion recovery tagging pulse. J Magn Reson Imaging 2005; 22:527–533.
27. Gouya H, Vignaux O, Sogni P, et al. Chronic liver disease: systemic and splanchnic venous flow mapping with optimized cine phase-contrast MR imaging validated in a phantom model and prospectively evaluated in patients. Radiology 2011; 261:144–155.
28. Wai CT, Greenson JK, Fontana RJ, et al. A simple noninvasive index can predict both significant fibrosis and cirrhosis in patients with chronic hepatitis C. Hepatology 2003; 38:518–526.
29. Gorka W, al Mulla A, al Sebayel M, Altraif I, Gorka TS. Qualitative hepatic venous Doppler sonography versus portal flowmetry in predicting the severity of esophageal varices in hepatitis C cirrhosis. AJR Am J Roentgenol 1997; 169:511–515.
30. Lipp MJ, Broder A, Hudesman D, et al. Detection of esophageal varices using CT and MRI. Dig Dis Sci 2011; 56:2696–2700.
31. Ernst O, Asnar V, Sergent G, et al. Comparing contrast-enhanced breath-hold MR angiography and conventional angiography in the evaluation of mesenteric circulation. AJR Am J Roentgenol 2000; 174:433–439.
32. Li FH, Hao J, Xia JG, Li HL, Fang H. Hemodynamic analysis of esophageal varices in patients with liver cirrhosis using color Doppler ultrasound. World J Gastroenterol 2005; 11:4560–4565.
33. Yzet T, Bouzerar R, Allart JD, et al. Hepatic vascular flow measurements by phase contrast MRI and doppler echography: a comparative and reproducibility study. J Magn Reson Imaging 2010; 31:579–588.
34. Stankovic Z, Csatari Z, Deibert P, et al. Normal and altered three-dimensional portal venous hemodynamics in patients with liver cirrhosis. Radiology 2012; 262:862–873.
35. François CJ, Srinivasan S, Schiebler ML, et al. 4D cardiovascular magnetic resonance velocity mapping of alterations of right heart flow patterns and main pulmonary artery hemodynamics in tetralogy of Fallot. J Cardiovasc Magn Reson 2012; 14:16.
36. Frydrychowicz A, Landgraf BR, Niespodzany E, et al. Four-dimensional velocity mapping of the hepatic and splanchnic vasculature with radial sampling at 3 tesla: a feasibility study in portal hypertension. J Magn Reson Imaging 2011; 34: 573–584.